Effects of Second Phase Morphology on Deep Drawability of TRIP-aided Dual-phase Sheet Steels*

Akihiko NAGASAKA** and Kazuhide WADA***

Effects of retained austenite parameters on the deep drawability in high-strength TRIP-aided dual-phase (TDP) sheet steels with different silicon and manganese contents were investigated. The deep drawability evaluated with a limiting drawing ratio (*LDR*) was affected by volume fraction of the retained austenite rather than by its stability and morphology. Namely, the higher the volume fraction of the retained austenite, the larger the strength – deep drawability balance, i.e., the product of tensile strength and *LDR*. The excellent deep drawability was caused by large local necking resistance at the cup wall just above the punch bottom due to "the transformation hardening" and "the stress relaxation" resulting from the strain-induced martensite transformation, as well as a low punch force of the shrinking flange.

Key words: Deep drawability; Retained austenite; Transformation-induced plasticity.

1. Introduction

A TRIP-aided dual-phase steel associated with the transformation-induced plasticity (TRIP)[1] of the retained austenite, or a TDP steel, possesses the excellent deep drawability of high-strength sheet steels which were recently developed for shock-safety and weight reduction of the automobile[2 – 5]. So, much research has been done to apply the steel to various automotive structural parts such as the impact parts and the suspension parts[6]. The deep drawability of the TDP steel is expected to be controlled by the retained austenite parameters (volume fraction, carbon concentration and morphology), in the same ways as the elongation[7 – 10], the stretch-formability[11, 12] and the stretch-flangeability[13 – 15]. However, there have been few investigations dealing with the deep drawability from such the point of view.

In the present study, the deep drawability of the TDP steels with different retained austenite parameters were examined. In addition, the relation between the deep drawability and the retained austenite parameters, as well as deformation characteristics on Swift cup forming, was investigated to propose the improving mechanism of deep drawability.

2. Experimental Procedure

The chemical composition of as-cold-rolled sheet steels of 1.2 mm in thickness used in this study is shown in Table 1. The steels were subjected to two types of heat treatments (Fig. 1) for changing the morphology of second phase and retained austenite. In Fig. 1, intercritical annealing for these steels was carried out at a given temperature ($T_{\alpha+\gamma}$), at which the volume fraction of the retained austenite becomes maximum[7]. Hereafter, the steels subjected to the heat treatment are called TYPE I and TYPE II steels, respectively.

Tensile tests were performed on an Instron type of tensile testing machine at a crosshead speed of 1

Table 1. Chemical composition of steels used (mass%).

Steel	C	Si	Mn	P	S	Al
A	0.21	1.51	1.00	0.015	0.0013	0.041
B	0.20	1.50	1.50	0.015	0.0012	0.041
C	0.20	1.49	1.99	0.015	0.0015	0.039
E	0.20	1.00	1.50	0.014	0.0013	0.038
F	0.18	2.00	1.50	0.015	0.0013	0.037
G	0.19	2.48	1.49	0.014	0.0013	0.036

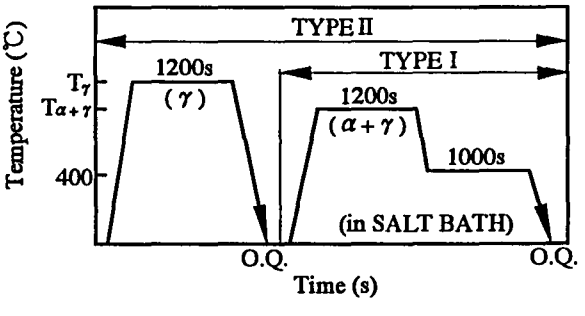

Fig. 1. Heat treatment diagram of TDP steels, in which "O.Q." represents quenching in oil and T_γ and $T_{\alpha+\gamma}$ are austenitizing and intercritical annealing temperatures, respectively.

* Retouch correction of JISSE-6; October 26 - 29, 1999
** Associate Professor, Department of Mechanical Engineering
*** First Technical Section
A part of this research was accomplished by the education research special expenditure of 1999 term.
Received October 29, 1999

mm/min, using JIS-13B-type tensile specimens.

Swift cup test was carried out on a universal plasticity testing machine. The deep drawability was evaluated with a limiting drawing ratio ($LDR = D_0/d_p$), where the D_0 and the d_p are a maximum blank diameter drawn out and a punch diameter, respectively. These die dimensions are illustrated in Fig. 2. The tests with disk specimens of $D_0 = 39$ to 45 mm in diameter were performed under a constant blank holding force of 10 kN and at a punch speed of about 200 mm/min. Prior to drawing test, a dry lubricant was coated on all the specimens.

The volume fraction of the retained austenite was quantified by X-ray diffractometry using MoK_α radiation (five peak method)[16]. In addition, the initial carbon concentration in the retained austenite ($C_{\gamma 0}$, mass%) was estimated from lattice parameter ($a_{\gamma 0}$, nm) measured from $(220)_\gamma$ diffraction peak of CrK_α radiation using the following equation[17].

$$a_{\gamma 0} = 0.35467 + 4.67 \times 10^{-3} \times C_{\gamma 0} \quad (1)$$

3. Results and Discussion

3.1. Structure and tensile properties

Fig. 3 shows (a and c) optical micrographs and (b and d) scanning electron ones of steel B with different second phase morphology, in which white phases in (a) and (c) represent the retained austenite. The optical micrographs were color etched using the LePara method[18] while the scanning electron micrographs

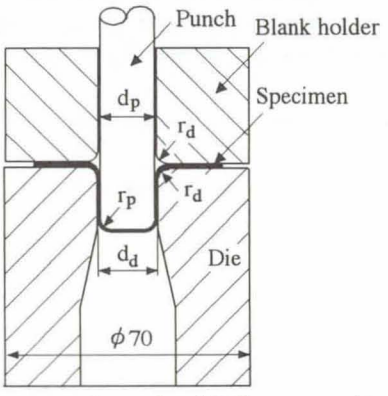

(d_p = 20.64 mm, r_p = 4 mm, d_d = 24.40 mm, r_d = 4 mm)

Fig. 2. Experimental apparatus for Swift cup test.

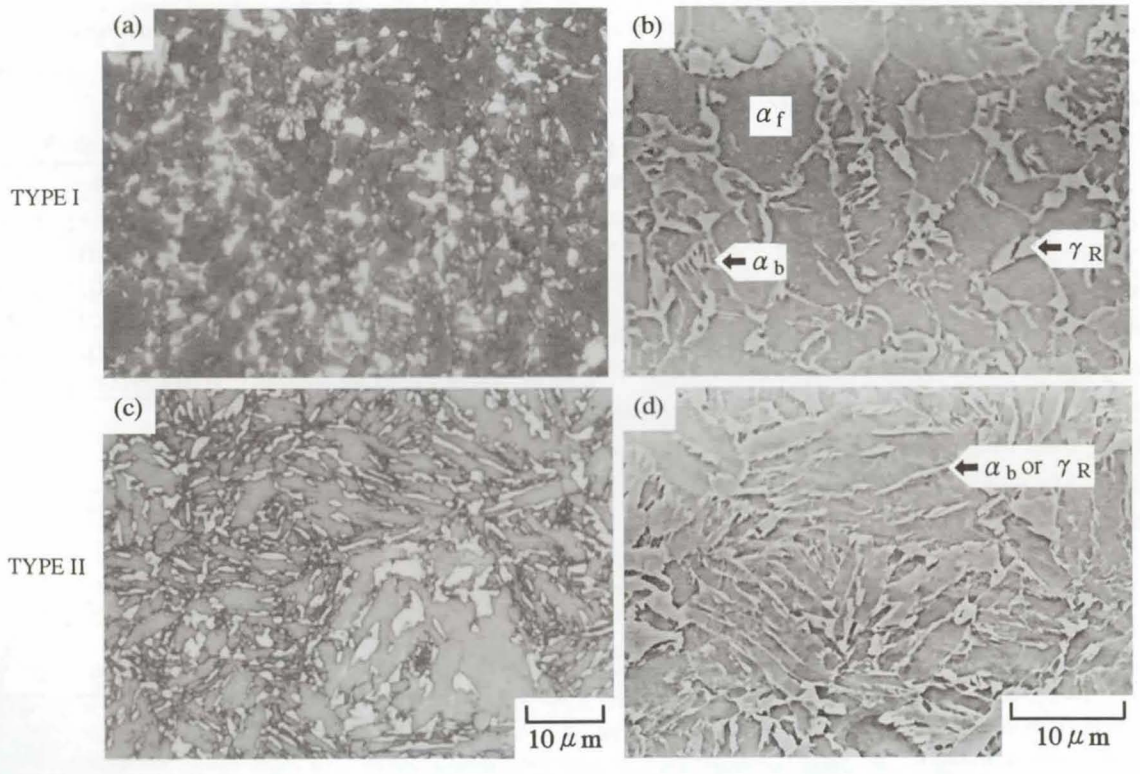

Fig. 3. Optical and scanning electron micrographs of steel B with (a and b) TYPE I or (c and d) TYPE II morphology, in which white phases in (a) and (c) represent retained austenite and "α_f", "α_b" and "γ_R" are ferrite matrix, bainite and retained austenite, respectively.

were etched in a 3% nital solution. The TYPE I and TYPE II steels can be classified as (a and b) a network structure along the ferrite grain boundary and (c and d) an isolated fine and acicular one, respectively.

The initial volumefraction of retained austenite ($f_{\gamma 0}$) increases and its carbon concen-tration ($C_{\gamma 0}$) decreases with increasing silicon and manganese contents for TYPE I and TYPE II steels, as listed in Table 2.

Tensile properties of the steels are also listed in Table 2. The tensile strength (*TS*) is in a wide range of 742 to 984 MPa and tends to increase with silicon and manganese contents. It is noteworthy that the TDP steels have extremely large total elongation (*TEl*) and high work hardening exponent (*n*-value), though the Lankford's value or *r*-value is below unity.

3.2. Deep drawability

Fig. 4 shows a comparison of *LDR* value as a function of tensile strength (*TS*) for TYPE I and TYPE II steels, accompanied with those of a ferrite – bainite dual-phase steel (BDP steel) and a ferrite – martensite dual-phase steel (MDP steel) without retained austenite[4, 5].

The TDP steels exhibit the best deep drawability of the high-strength sheet steels, despite low *r*-value less than unity. However, if the deep drawability was evaluated with the strength – deep drawability balance, i.e., the product of *TS* and *LDR*, the TDP steels with high silicon and/or manganese contents possess larger *TS*×*LDR* values than the other TDP steels. From Figs. 5 and 6, it is found that the *TS*×*LDR* value represents a positive correlation with the volume fraction of the retained austenite rather than its stability and morphology, unlike in cases of the elongation, the stretch-

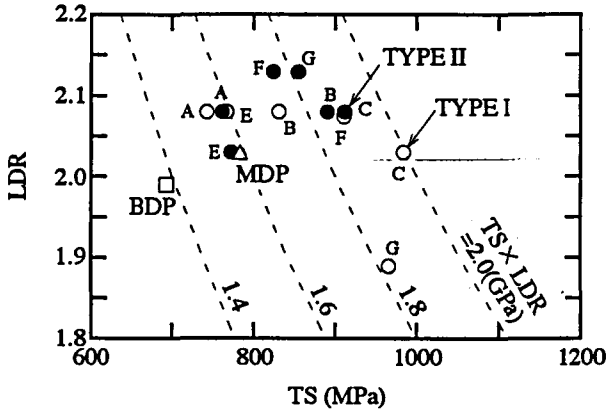

Fig. 4. Comparison of limiting drawing ratio (*LDR*) of TDP, $\alpha_f + \alpha_b$ dual-phase (BDP) and $\alpha_f + \alpha_m$ dual-phase (MDP) steels as a function of tensile strength (*TS*).

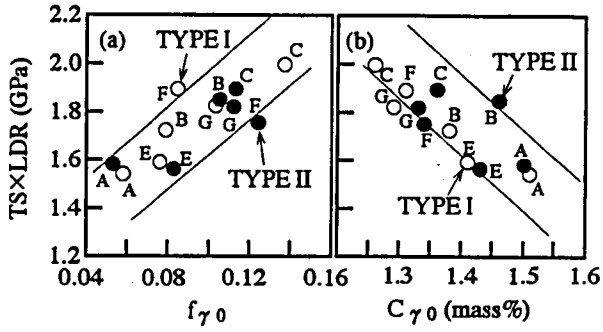

Fig. 5. Correlation between strength – deep drawability balance (*TS*×*LDR*) and retained austenite parameters in TDP steels.

Table 2. Retained austenite characteristicsand tensile properties.

Steel	TYPE	$f_{\gamma 0}$	$C_{\gamma 0}$ (mass%)	YS (MPa)	TS (MPa)	UEl (%)	TEl (%)	YR	ε_f	n	r	HV_0
A		0.058	1.51	470	742	27.2	32.3	0.63	0.84	0.25	0.94	222
B		0.079	1.38	527	831	31.4	35.8	0.63	0.67	0.26	0.89	240
C	I	0.137	1.26	516	984	20.4	22.9	0.52	0.56	0.23	0.84	295
E		0.076	1.41	494	767	24.6	29.0	0.64	0.74	0.23	0.92	248
F		0.085	1.31	517	911	27.8	31.9	0.57	0.59	0.30	0.87	273
G		0.103	1.29	468	966	24.5	28.8	0.48	0.43	0.28	0.89	282
A		0.053	1.50	490	761	18.9	23.4	0.64	0.85	0.20	0.78	247
B		0.105	1.46	629	890	27.9	32.4	0.71	0.81	0.19	0.87	265
C	II	0.113	1.36	623	912	26.2	31.8	0.68	0.74	0.21	0.84	293
E		0.083	1.43	571	772	17.2	22.1	0.74	0.74	0.17	0.82	261
F		0.124	1.34	565	824	32.1	36.7	0.60	0.65	0.18	0.87	273
G		0.112	1.33	610	855	21.5	25.6	0.71	0.60	0.25	0.86	292

$f_{\gamma 0}$: initial volume fraction of the retained austenite, $C_{\gamma 0}$: initial carbon concentration in the retained austenite, *YS*: 0.2% offset proof stress or yield stress, *TS*: tensile strength, *UEl*: uniform elongation, *TEl*: total elongation, *YR*: yield ratio (=*YS*/*TS*), ε_f: fracture ductility, *n*: work hardening exponent (ε =5 – 15%), *r*: *r*-value (ε =10%) and HV_0: initial Vickers hardness (load=9.81N).

formability[12] and the stretch-flangeability[14, 15]. Therefore, a large amount of retained austenite can be principally considered to result in the above mentioned excellent deep drawability.

3.3. Improving mechanism of deep drawability

The deep drawability is in general controlled by a ratio of critical fracture force (P_{cr}) on the cup wall just above the radius of the punch to maximum punch force (P_{max}), i.e., the equivalent critical fracture force (P_{max}/P_{cr})[19]. Namely, the lower the P_{max}/P_{cr} value, the larger the deep drawability. The P_{cr} can be estimated by[3]

$$P_{cr} = \pi d_p t_0 \sigma_p \tag{2}$$

$$\sigma_p = (2/\sqrt{3}) \cdot [\sqrt{3}(1+r)/2\sqrt{1+2r}]^{1+n} \cdot TS \tag{3}$$

where d_p, t_0, σ_p, n, r and TS represent punch diameter, thickness, fracture stress in plane strain[19], n-value, r-value and tensile strength, respectively.

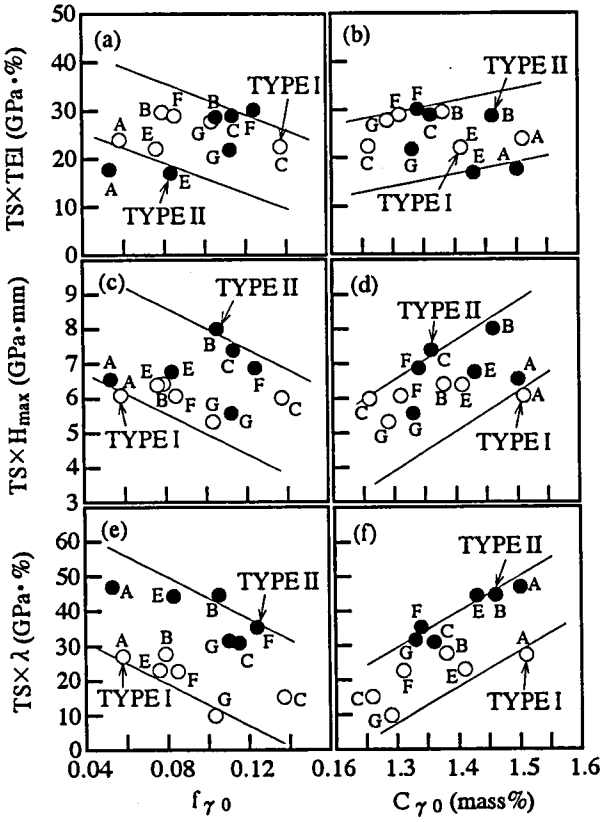

Fig. 6. Correlations between strength−ductility balance ($TS\times TEl$), strength−stretch-formability balance ($TS\times H_{max}$) and strength−stretch-flangeability balance ($TS\times\lambda$) and retained austenite parameters in TDP steels.

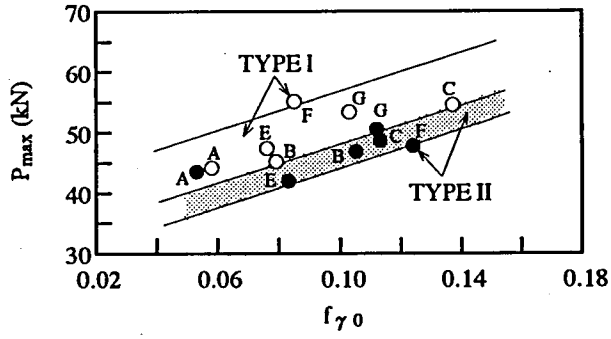

Fig. 7. Variation in maximun punch force (P_{max}) with initial volume fraction of retained austenite ($f_{\gamma 0}$) of TDP steels (DR= 1.89).

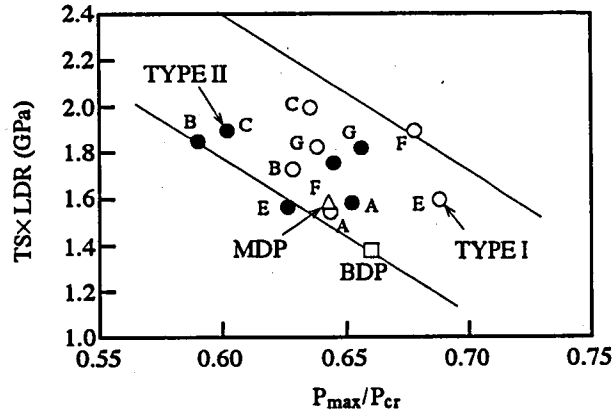

Fig. 8. Relation between strength−deep drawability balance ($TS\times LDR$) and equivalent critical fracture force (P_{max}/P_{cr}).

Fig. 7 shows a variation in maximun punch force (P_{max}) with the volume fraction of the retained austenite. And, Fig. 8 shows a relation between the strength−deep drawability balance and the equivalent critical fracture force for TYPE I and TYPE II steels. The $TS\times LDR$ values appeared to be increased with a decrease in the P_{max}/P_{cr}. This indicates that the deep drawability of the TDP steels is enhanced by the increased critical fracture force. The deep drawability was also increased with increasing retained austenite content, as shown in Fig. 5. Therefore, the excellent deep drawability is considered to be caused by large local necking resistance at the cup wall just above the punch bottom due to "the transformation hardening" and "the stress relaxation" resulting from the strain-induced martensite transformation, as well as a low drawing force of the shrinking flange.

4. Conclusions

The effects of retained austenite parameters and second phase morphology on the deep drawability of the TRIP-aided dual-phase steels were investigated. The results were summarized as follows.

1) The TDP steels possessed the best deep drawability of the high-strength sheet steels, despite low *r*-value less than unity.

2) The deep drawability was controlled by the volume fraction of the retained austenite rather than by its stability and morphology. Namely, the higher the volume fraction of the retained austenite, the larger the strength – deep drawability balance.

3) The excellent deep drawability was caused by large local necking resistance at the cup wall just above the punch bottom due to the transformation hardening and the stress relaxation resulting from the strain-induced martensite transformation, as well as a low drawing force of the shrinking flange.

Acknowledgements

The authors wish to thank The Iron and Steel Institute of Japan and the education research special expenditure of 1999 term in Nagano National College of Technology for their financial supports.

References

[1] V. F. Zackay, E. R. Parker, D. Fahr and R. Busch: *Trans. Am. Soc. Met.*, **60** (1967), 252.

[2] O. Matsumura, T. Ohue and T. Amaike: *Tetsu-to-Hagane*, **79** (1993), 209.

[3] S. Hiwatashi, M. Takahashi, T. Katayama and M. Usuda: *J. Jpn. Soc. Technol. Plast.*, **35** (1994), 1109.

[4] A. Nagasaka, K. Sugimoto and M. Kobayashi: Proc. of the Asian Conf. on Heat Treatment of Materials, ed. by C. Zailiang et al., China Machine Press, Beijing, (1998), 219.

[5] A. Nagasaka, K. Sugimoto, M. Kobayashi and S. Hashimoto: *Tetsu-to-Hagane*, **85** (1999), 552.

[6] Y. Ojima, Y. Shiroi, Y. Taniguchi and K. Kato: SAE Tech. Pap. Ser., #980954, (1998), 39.

[7] O. Matsumura, Y. Sakuma and H. Takechi: *Trans. Iron Steel Inst. Jpn.*, **27** (1987), 570.

[8] K. Sugimoto, M. Kobayashi and S. Hashimoto: *Metall. Trans. A*, **23A** (1992), 3085.

[9] K. Sugimoto, N. Usui, M. Kobayashi and S. Hashimoto: *ISIJ Int.*, **32** (1992), 1311.

[10] K. Sugimoto, M. Misu, M. Kobayashi and H. Shirasawa: *ISIJ Int.*, **33** (1993), 775.

[11] O. Matsumura, Y. Sakuma, Y. Ishii and J. Zhao: *ISIJ Int.*, **32** (1992), 1110.

[12] K. Sugimoto, M. Kobayashi, A. Nagasaka and S. Hashimoto: *ISIJ Int.*, **35** (1995), 1407.

[13] A. Nagasaka, K. Sugimoto, M. Kobayashi and S. Hashimoto: *Tetsu-to-Hagane*, **83** (1997), 335.

[14] A. Nagasaka, K. Sugimoto, M. Kobayashi and H. Shirasawa: *Tetsu-to-Hagane*, **84** (1998), 218.

[15] K. Sugimoto, A. Nagasaka, M. Kobayashi and S. Hashimoto: *ISIJ Int.*, **39** (1999), 56.

[16] H. Maruyama: *J. Jpn. Soc. Heat Treat.*, **17** (1977), 198.

[17] Z. Nishiyama: Martensite Transformation, Maruzen, Tokyo, (1971), 13.

[18] E. Girault, P. Jacques, Ph. Harlet, K. Mols, J Van Humbeek, E. Aernoudt and F. Delauuay: *Mater. Charact.*, **40** (1998), 111.

[19] M. Usuda, Y. Ishii, S. Ujihara and T. Sakamoto: *36th Annual Meeting of J. Jpn. Soc. Technol. Plast.*, (1985), 317.